

## Fundamental Limit of Nonscaling Fixed-Field Alternating-Gradient Accelerators

S. Y. Lee

*Department of Physics, Indiana University, Bloomington, Indiana 47405, USA*  
*GSI, Darmstadt, D64291, Germany*

(Received 14 March 2006; published 6 September 2006)

*Systematic* nonlinear space-charge resonances may cause substantial emittance growth in the nonscaling fixed-field alternating-gradient (FFAG) accelerators. To avoid systematic nonlinear space-charge resonances, the phase advance of each nonscaling FFAG cell must avoid  $\pi/2$  and  $\pi/3$ . Using multiparticle numerical simulations, we empirically obtain a minimum tune ramp rate vs the systematic 4th order space-charge resonance strength. We also find that the emittance growth obeys a simple scaling property when the betatron tunes cross the linear half-integer and sum resonances.

DOI: [10.1103/PhysRevLett.97.104801](https://doi.org/10.1103/PhysRevLett.97.104801)

PACS numbers: 29.27.-a, 41.75.-i, 52.59.Sa

There is a recent revival of interests in using the fixed-field alternating-gradient accelerators (FFAG) for proton drivers [1], which may find applications in muon colliders, neutrino factory, neutron sources, energy amplifiers, etc. “The FFAG research in the United States focuses on the nonscaling design” [2,3] that requires a much smaller magnet aperture. Unfortunately, the betatron tunes of the nonscaling FFAG cannot be maintained at a value within two integers. The betatron tunes decrease because the focusing field is kept nearly constant while the beam momentum increases at a rate of  $\frac{d\nu}{dn} \approx -\nu \frac{dE/dn}{\beta^2 E}$ , where  $dE/dn$  is the energy gain in one revolution. Hereafter, the tune-ramp rate refers to the rate change of the “bare” betatron tunes per revolution. Even if the energy gain per revolution could reach 1 MeV, the tune-ramp rate would be less than 0.02. The FFAG accelerator may encounter many technical challenges in rf, magnet, and vacuum technologies. However, the most fundamental issue is the emittance blowup due to the self-space-charge force, which cannot be corrected. Here the rms beam emittance is defined as the rms phase-space area occupied by the beam particles.

Many sources cause emittance growth in circular accelerators, including the half-integer stop band that can perturb the beam envelope function [4–6], the Montague resonance [7], and the sum resonance induced by the random skew-quadrupole-field [8]. Although there are some studies on the effects of resonance crossing in the FFAG [3,9], these works examine only nonsystematic resonances, which are in principle correctable. This Letter intends to study an emittance growth mechanism caused by the modulation of the self space-charge force due to the repeated beam size variation in accelerator lattice cells. Even if the FFAG accelerator is perfectly designed and constructed, a sizable emittance dilution can occur when the betatron tunes (spectra of beam motion) encounter resonance conditions driven by the self space-charge force.

To study the emittance growth, we construct a multiparticle simulation program to simulate the evolution of

beam emittances. The accelerator lattice is  $P = 24$  FODO cells, made of the focusing and defocusing quadrupoles separated by bending dipoles or drift spaces. As the beam particles are injected and accumulated, particles in the accelerator experience a space-charge force proportional to the beam intensity. Our numerical-simulation algorithm [8] consists of (1) a linear transport for phase-space coordinates in a half FODO cell by a linear transfer matrix, (2) a space-charge force kick to the phase-space coordinates, (3) a linear transport by the second half of the FODO cell transfer matrix, and (4) a space-charge force kick at the end of the basic FODO cell. This procedure is carried out for 24 FODO cells in one revolution.

With a Gaussian charge distribution  $\rho(x, z) = \frac{Ne}{2\pi\sigma_x\sigma_z} \times \exp\{-\frac{x^2}{2\sigma_x^2} - \frac{z^2}{2\sigma_z^2}\}$ , the transverse space-charge potential is [10]

$$V(x, z) = \frac{K_{sc}}{2} \int_0^\infty \frac{-1 + \exp\{-\frac{x^2}{2\sigma_x^2+t} - \frac{z^2}{2\sigma_z^2+t}\}}{\sqrt{(2\sigma_x^2+t)(2\sigma_z^2+t)}} dt, \quad (1)$$

where  $\sigma_x$  and  $\sigma_z$  are the horizontal and vertical rms beam radii,  $N = N_B/(\sqrt{2\pi}\sigma_s)$  is the charge per unit length,  $N_B$  is the number of particles in a bunch,  $\sigma_s$  is the longitudinal rms bunch length,  $K_{sc} = 2Nr_0/(\beta^2\gamma^3)$  is the generalized space-charge perveance, and  $r_0 = 1.5347 \times 10^{-18}$  m is the classical radius of the proton. The horizontal rms beam radius is composed of both the betatron and off-momentum contributions.

Because of the space-charge potential, each particle experiences a space-charge kick:

$$\Delta x' = -\frac{\partial V}{\partial x} l \approx \frac{K_{sc} l}{\sigma_x(\sigma_x + \sigma_z)} x \exp\left\{-\frac{x^2 + z^2}{(\sigma_x + \sigma_z)^2}\right\},$$

$$\Delta z' = -\frac{\partial V}{\partial z} l \approx \frac{K_{sc} l}{\sigma_z(\sigma_x + \sigma_z)} z \exp\left\{-\frac{x^2 + z^2}{(\sigma_x + \sigma_z)^2}\right\},$$

where  $l$  is the length of the half cell, and the exponential form is obtained by expanding the space-charge potential of Eq. (1) up to the second order in round beam geometry and exponentiated to produce zero tune shift for large

amplitude particles. The linear space-charge tune shift is  $\Delta\nu_{x,sc} = \frac{1}{4\pi} \oint \frac{\beta_x(s)K_{sc}}{\sigma_x(\sigma_x + \sigma_z)} ds$ ,  $\Delta\nu_{z,sc} = \frac{1}{4\pi} \oint \frac{\beta_z(s)K_{sc}}{\sigma_z(\sigma_x + \sigma_z)} ds$ , where  $\beta_x(s)$  and  $\beta_z(s)$  are the betatron amplitude functions, and  $\Delta\nu_{sc}$  is the horizontal or the vertical linear space-charge tune shift at initial beam emittances.

The space-charge force is approximated by 48 localized kicks per revolution in our numerical model. The rms beam radii calculated from the multiparticle phase-space distribution are used for space-charge kicks in the next revolution. Although the distribution function may become non-Gaussian, our space-charge kick remains in the Gaussian beam approximation. This simplified space-charge model is implemented to speed up calculations for systematic parametric study. When the accelerator is free from random errors, only systematic resonances can affect particle motion. Systematic nonlinear space-charge resonances are  $4\nu_x = P$ ,  $4\nu_z = P$ ,  $2\nu_x + 2\nu_z = P$ ,  $6\nu_x = P$ , etc., where  $P = 24$  in our model.

To study the effect of the systematic nonlinear space-charge force on the nonscaling FFAG, we consider a beam with 100 injection turns and an initial rms emittance of  $8.5\pi$  mm mrad such that  $\Delta\nu_{x,sc} \approx \Delta\nu_{z,sc} = 0.109$ . The left plots of Fig. 1 show the evolution of the betatron tunes and the rms beam emittances for the cases, where the bare betatron tunes are linearly ramped downward from (6.25, 6.20) to (5.85, 5.80) [see the blue color points], upward from (5.85, 5.80) to (6.25, 6.20) [see the red color points], and upward or downward between (6.85, 6.80) and (7.25, 7.20) [see the green color curves] from 200 to 1000 revolutions.

Note that the emittance growth is severe for the down ramp through the systematic space-charge resonance, because the betatron tunes of small-amplitude particles stay longer at the resonance (see the top-left plot of Fig. 1; see also Ref. [11]). The normalized phase-space distributions

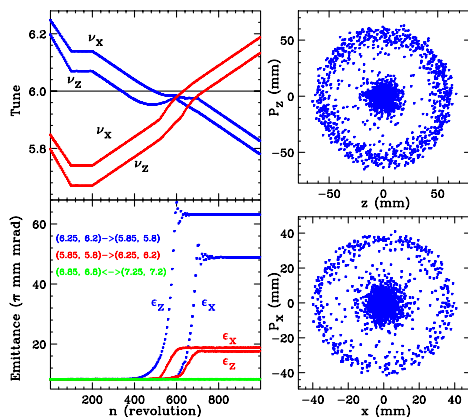


FIG. 1 (color online). Left plots: The evolution of the small-amplitude betatron tunes and the normalized emittances vs revolution numbers for a beam with  $\Delta\nu_{sc} = 0.109$  while ramping the bare betatron tunes through the systematic space-charge nonlinear resonances. Right plots: the normalized phase-space maps at the end of down ramp.

at 1000 revolution are shown in the right plots of Fig. 1. When the beam particle approaches the  $4\nu_x = 24$  and  $4\nu_z = 24$  resonances, small-amplitude particles are transported and trapped onto the 4th order resonance islands, and decohere into a ring in the phase space as shown in the right plots of Fig. 1. Ramping through a nonsystematic resonance does not cause any emittance growth (see the green curves in Fig. 1). Existence of the 4th order systematic space-charge resonance islands is known to exist in the self-consistent space-charge model calculations [12], numerical simulations and experimental measurements at the KEK PS [13,14].

We define the emittance growth factor (EGF) as the ratio of the final emittance to the initial. The EGF does not depend on the horizontal or vertical emittance. When crossing a horizontal resonance, the EGF corresponds to the horizontal emittance growth, and vice versa. The bottom plot of Fig. 2 shows the EGF as a function of the tune-ramp rate:  $\Delta\nu/\Delta n$ . Note that the EGF shows a power law, i.e., the EGF is proportional to  $(\Delta\nu/\Delta n)^a$  in the low crossing rate regime, where  $a \approx -0.62$ . The EGF depends also on the strength of the space-charge force. Using the  $\Delta\nu_{sc}$  as the scaling parameter, the top plot of Fig. 2 shows the EGF as a function of  $\Delta\nu_{sc}$  for fixed tune-ramp rates.

The 4th order space-charge potential in Eq. (1) can be expanded in action-angle phase-space coordinates:  $V_4(J_x, J_z, \psi_x, \psi_z, \theta) \approx G_{4,0,l} J_x^2 \cos(4\psi_x - l\theta + \chi_x) + G_{0,4,l} J_z^2 \cos(4\psi_z - l\theta + \chi_z) + G_{2,2,l} J_x J_z \cos(2\psi_x + 2\psi_z - l\theta + \chi_+) + G_{2,-2,l} J_x J_z \cos(2\psi_x - 2\psi_z - l\theta + \chi_-)$ , where  $(J_x, \psi_x)$  and  $(J_z, \psi_z)$  are the horizontal and vertical action-angle coordinates, and  $\chi$ 's are the phase of the resonance strength parameter. The resonance strength  $G_{m,n,l}$  depends on the lattice design and the space-charge permeance, [15]. For a beam with equal emittances  $\epsilon = \epsilon_x = \epsilon_z$ , one finds  $G_{m,n,l} \approx g_{m,n,l} [K_{sc} C / (8\pi\epsilon^2)]$ , where  $C$  is the circumference of the accelerator, the dimensionless reduced resonance strength  $g_{m,n,l}$  depends essentially on

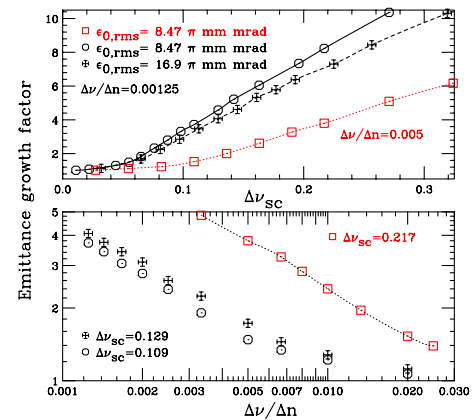


FIG. 2 (color online). Top: The EGF, defined as the ratio of the final emittance to the initial, vs  $\Delta\nu_{sc}$  for crossing  $4\nu_x = P$  or  $4\nu_z = P$  resonance. Bottom: The EGF vs the resonance crossing rate,  $\Delta\nu/\Delta n$ .

the accelerator lattice functions, and  $K_{sc}C/(8\pi\epsilon) \approx \Delta\nu_{sc}$ . A larger variation in the betatron amplitude functions gives a larger reduced resonance strength.

Define the critical tune-ramp rate as the extrapolation of each EGF curve cutting the horizontal axis in the bottom plot of Fig. 2. At the critical tune-ramp rate, the EGF is about 1.2. Figure 3 shows the critical tune-ramp rate vs the reduced resonance strength  $g_{0,4,l}$ , obtained by varying the betatron amplitude functions at the space-charge kick locations. The error bar reflects the uncertainty in the linear extrapolation. Since the EGF curve has a sharper turn for a smaller  $\Delta\nu_{sc}$ , the corresponding error bar is smaller. Given  $\Delta\nu_{sc}$  and  $d\nu/dn$ , one obtains the maximum tolerable reduced 4th order resonance strength, which constrains the accelerator lattice design.

Besides these systematic space-charge resonances, random errors play an important role in particle beam dynamics. Since the dipole field errors affect the closed orbit, which is relevant to the beam emittance at injection, we assume that the closed orbit is properly corrected. The random quadrupoles break the superperiodicity, and produce half-integer stop bands. The random skew quadrupoles introduce both the sum and difference coupling resonances, found to be important in beam-emittance growth in fast ramping accelerators [8].

For the random quadrupole error, the stop-band width, defined as the Fourier amplitude of quadrupole-field error at the  $p$ th harmonic, is

$$G_p = \frac{1}{2\pi} \oint \beta(s) \Delta K(s) e^{-ip\phi(s)} ds, \quad (2)$$

where  $\beta(s)$  is either the horizontal or vertical betatron amplitude function,  $\Delta K(s)$  is the quadrupole-field error,  $\phi(s) = (1/\nu) \int_0^s ds/\beta(s)$ , and  $s$  is the longitudinal coordinate. When the betatron tune  $\nu$  of a particle sits at  $p/2$ , the action of the particle will grow exponentially as  $\exp\{2\pi|G_p|n\}$ , where  $n$  is the revolution number. Random skew quadrupoles produces both sum and difference resonances. When the betatron tunes are ramped

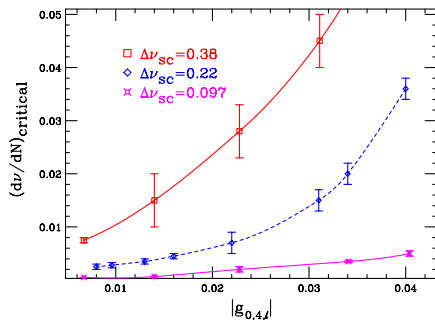


FIG. 3 (color online). The critical resonance crossing rate,  $(\Delta\nu/\Delta n)_{\text{critical}}$ , defined as the extrapolation of the EGF cutting the horizontal axis in the bottom plot of Fig. 2, is shown as a function of the reduced resonance strength  $g_{0,4,l}$  for crossing  $4\nu_x = P$  resonance.

through many integers, the sum resonance is unavoidable. The stop-band width of the sum resonance is the Fourier amplitude of the skew-quadrupole error field  $A(s)$ : [5],

$$G_{1,1,l} = \frac{1}{2\pi} \oint \sqrt{\beta_x(s)\beta_z(s)} A(s) e^{i\chi_{1,1,l}(s)} ds, \quad (3)$$

where  $\beta_x(s)$  and  $\beta_z(s)$  are the horizontal and the vertical betatron amplitude functions,  $\chi_{1,1,l}(s) = \psi_x(s) + \psi_z(s) - (\nu_x + \nu_z - l)s/R$  is the sum-resonance phase function,  $\psi_x(s)$  and  $\psi_z(s)$  are the betatron phase functions, and  $R$  is the mean radius of the accelerator. When the betatron tunes of a particle sit on a sum resonance, both the horizontal and vertical actions will grow as  $\exp\{2\pi|G_{1,1,l}|n\}$ .

Let the stop-band width be  $g = |G_p|$  or  $g = |G_{1,1,l}|$ . The EGF for passing through a resonance is approximately  $\exp\{g\Delta n\}$ , where  $\Delta n$  is the number of revolutions that the tunes of beam particles are inside the stop-band width. Since  $\Delta n \sim g/(d\nu/dn)$ , the EGF becomes

$$\text{EGF} = \exp\{\lambda 2\pi g^2/(d\nu/dn)\}. \quad (4)$$

The EGF is numerically obtained by adding the random quadrupole and skew-quadrupole kicks to each half cell [8]. We prepare a beam with  $\Delta\nu_{sc} = 0.217$ . The bare betatron tunes are linearly ramped from (6.85, 7.80) to (5.85, 6.80) in 50 revolutions. The horizontal EGF is about 1.5 for the  $4\nu_x = P$  structure resonance. The EGF is separately obtained for quadrupole and skew-quadrupole errors which are randomly generated by different random seeds. A stop-band width is then calculated from each error seed. Figure 4 shows the EGF as a function of the stop-band width for both the quadrupole and skew-quadrupole errors.

Figure 5 shows  $\ln(\text{EGF})$  as a function of  $2\pi g^2/(d\nu/dn)$  for  $d\nu/dn = 0.01$  and  $0.02$  in the down-ramp condition. The parameter  $\lambda$  is larger than 1 in the down ramp because the betatron tunes of small-amplitude particles stay longer at the resonance resulting from the space-charge tune shift. The slope gives  $\lambda \approx 3.5$  for the sum resonance, and 1.5 for the half-integer stop bands (shown as dashed lines in Fig. 5). The slope  $\lambda$  depends also slightly on the space-charge tune shift parameter  $\Delta\nu_{sc}$ .

In conclusion, we use the rms space-charge potential model to carry out parametric study on emittance growth due to systematic space-charge resonances. Even for a perfectly designed and constructed FFA, the systematic fourth order nonlinear space-charge resonances at  $4\nu_x = P$  and  $4\nu_z = P$ , and the 6th order systematic nonlinear resonance crossing at  $6\nu_x = P$  and  $6\nu_z = P$  can cause substantial emittance growth. Using multiparticle numerical simulations, we empirically obtain a minimum (critical) tune-ramp rate vs the resonance strength when crossing the systematic 4th order space-charge resonance. To avoid the 4th and 6th order systematic resonances, the phase advance of each periodic cell should avoid phase advance  $\pi/2$  or  $\pi/3$  per cell. Thus the momentum acceptance of the non-scaling FFA accelerator may be restricted. For a given tune-ramp rate, we can find a critical systematic 4th order

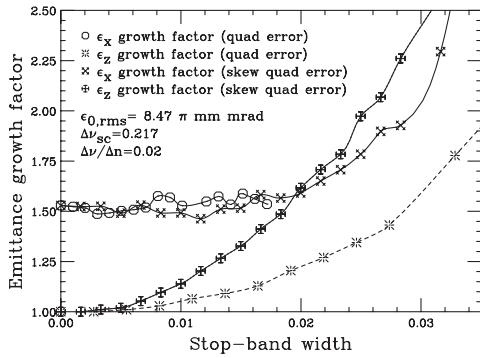


FIG. 4. The EGF is plotted as a function of the stop-band width for the random quadrupole and skew-quadrupole errors. The EGF obeys the scaling property:  $\exp\{\lambda 2\pi g^2/(d\nu/dn)\}$ , where  $\lambda$  is a constant,  $g$  is the stop-band width, and  $d\nu/dn$  is the tune-ramp rate. The EGF for the horizontal plane is dominated by the crossing of the systematic space-charge resonance at  $4\nu_x = P$ . Since the vertical tune does not cross the systematic space-charge resonance, its EGF arises solely from the random errors. The random seed used in the quadrupole error happens to produce the stop-band widths (0.017, 0.047) for the horizontal and vertical planes. The  $\epsilon_x$  growth factor (shown as circle symbols) stops at a stop-band width of about 0.017, because the vertical EGF becomes 3.08 and beam loss occurs.

space-charge resonance strength, which can be reduced by designing a smoother beam envelope function.

In reality, the linear random imperfections such as the dipole field errors, quadrupole-field errors, and skew quadrupole-field errors are important in emittance growth [8]. Emittance growth is inevitable if the tune is ramped through integer and half-integer resonances, unless stop band correction is implemented. The EGF can be expressed as  $\exp\{\lambda 2\pi g^2/(d\nu/dn)\}$ , where  $g$  is the stop-band width,  $d\nu/dn$  is the tune-ramp rate, and  $\lambda$  is a constant.

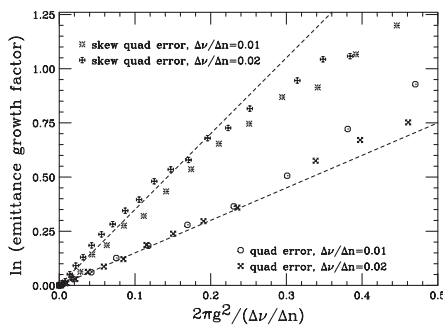


FIG. 5. The  $\ln(\text{emittance growth factor})$  for random quadrupole or skew-quadrupole errors is shown as a function of  $2\pi g^2/(d\nu/dn)$ , where  $g$  is the resonance stop-band width,  $d\nu/dn = 0.01, 0.02$  is the tune-ramp rate. The slope is the parameter  $\lambda$ . We find  $\lambda \approx 3.5$  for the sum resonances, and 1.5 for the half-integer stop bands (see dashed lines). The scaling law works well for  $d\nu/dn \geq 0.1$ . At a lower tune-ramp rate, the EGF may grow faster than exponential. The EGF due to systematic space-charge resonances is excluded in this plot.

The EGF scaling law sets tolerances on quadrupole-field error and quadrupole roll in the accelerator.

Our analysis is also applicable to the FFAG for the acceleration of muons. Since the mass of muon is about one fifth of the proton mass, the acceleration rate for muon is much higher, and the corresponding tune-ramp rate is much higher. Thus our analysis does not pose serious limitations to FFAG for muon acceleration.

This work is supported in part by Grants from the U.S. Department of Energy under Contract No. DE-FG0292ER40747 and the National Science Foundation NSF No. PHY-0552389. I also thank support from the Indiana University, USA and the Humboldt Foundation in Germany.

- [1] J.S. Berg *et al.*, in *Proceedings of the 17th Cyclotron Conference, Tokyo, Japan, 2004*, <http://www.jacow.org/>.
- [2] A. Ruggiero, BNL BNL AP-Technote: C-A/AP/#219, 2005.
- [3] J.S. Berg *et al.*, *Phys. Rev. ST Accel. Beams* **9**, 011001 (2006).
- [4] F.J. Sacherer, Ph.D. Thesis, UC Berkeley [Report No. UCRL-18454, UC Berkeley, 1968].
- [5] S.Y. Lee, *Accelerator Physics* (World Scientific, Singapore, 2004), 2nd ed.
- [6] S. Cousineau, Ph.D. Thesis, Indiana University, 2002; S. Cousineau *et al.*, *Phys. Rev. ST Accel. Beams* **6**, 034205 (2003).
- [7] B.W. Montague, CERN CERN-Report No. 68-38, 1968; I. Hofmann *et al.*, AIP Conf. Proceedings No. 773 (AIP, New York, 2004), p. 169; I. Hofmann *et al.*, *Proceedings of the 2005 Particle Accelerator Conference* (IEEE, New York, 2005), p. 330.
- [8] X. Huang *et al.*, *Phys. Rev. ST Accel. Beams* **9**, 014202 (2006).
- [9] A. Chao and M. Month, *Nucl. Instrum. Methods* **121**, 129 (1974); M. Aiba and S. Machida, *Proceedings of the European Particle Accelerator Conference 2004* (EPAC, Luzerne, Switzerland, 2004), p. 2119.
- [10] S. Kheifets, PETRA Note 119 (1976).
- [11] I. Hofmann and K. Beckert, *IEEE Trans. Nucl. Sci.* **NS-32**, 2264 (1985), <http://www.jacow.org/>.
- [12] Oliver Boine-Frankenheim (private communications); see also, I. Hofmann, G. Franchetti, and A. Fedotov, AIP Conf. Proceedings 642 (AIP, New York, 2002), p. 248.
- [13] S. Machida, *Nucl. Instrum. Methods Phys. Res., Sect. A* **384**, 316 (1997).
- [14] S. Igarashi *et al.*, *Proceedings of the Particle Accelerator Conference 2003* (IEEE, New York, 2003), p. 2610.
- [15] The space-charge potential for the  $x^2z^2$  term is normally uniform along the accelerator. Since the Fourier transform of a constant at a nonzero harmonic is zero, the resonance strength of  $2\nu_x + 2\nu_z = P$  is small. On the other hand, the Montague resonance strength at  $2\nu_x - 2\nu_z = 0$  is given by the zeroth harmonic of the  $x^2z^2$  term in the space-charge potential; its strength is large. But, we can easily design the accelerator lattice to avoid the Montague resonance condition.